



Published in final edited form as:

*Circ Heart Fail.* 2020 January ; 13(1): e006525. doi:10.1161/CIRCHEARTFAILURE.119.006525.

## Long Noncoding RNA *Ahit* Protects Against Cardiac Hypertrophy through SUZ12-Mediated Downregulation of MEF2A

Junyi Yu, M.D.<sup>1,\*</sup>, Yang Yang, M.S.<sup>1,\*</sup>, Zaicheng Xu, M.D, Ph.D.<sup>1,\*</sup>, Cong Lan, M.D<sup>1</sup>, Caiyu Chen, B.S<sup>1</sup>, Chuanwei Li, M.D, PhD<sup>1</sup>, Zhi Chen, M.D<sup>1</sup>, Cheng Yu, M.D<sup>1</sup>, Xuewei Xia, M.S<sup>1</sup>, Qiao Liao, M.S<sup>1</sup>, Pedro A. Jose, M.D, Ph. D<sup>2</sup>, Chunyu Zeng, M.D, Ph.D<sup>1,3</sup>, Gengze Wu, M.D, PhD<sup>1</sup>

<sup>1</sup>Department of Cardiology, Chongqing Institute of Cardiology, Chongqing Cardiovascular Clinical Research Center, Daping Hospital, The Third Military Medical University, Chongqing, P.R. China

<sup>2</sup>Division of Renal Disease & Hypertension, Departments of Medicine and Pharmacology/Physiology. The George Washington University School of Medicine and Health Sciences, Washington, DC.

<sup>3</sup>Cardiovascular Research Center, Chongqing College, University of Chinese Academy of Sciences, Chongqing, P.R. China

### Abstract

**Background**—Long non-coding RNA (lncRNA) can regulate various physiological and pathological processes through multiple molecular mechanisms *in cis* and *in trans*. However, the role of lncRNAs in cardiac hypertrophy is yet to be fully elucidated.

**Methods**—A mouse lncRNA microarray was used to identify differentially expressed lncRNAs in the mouse hearts following aortic constriction (TAC)-induced pressure-overload comparing to the Sham operated samples. The direct impact of one lncRNA, *Ahit*, on cardiomyocyte hypertrophy was characterized in neonatal rat cardiomyocytes in response to phenylephrine by targeted knockdown and over-expression. The *in vivo* function of *Ahit* was analyzed in mouse hearts by using cardiac specific AAV9-shRNA to knockdown *Ahit* in combination with TAC. Using catRAPID program, an interaction between *Ahit* and SUZ12 was predicted and validated by RNA-immunoprecipitation and immunoblotting following RNA pull-down. Chromatin-immunoprecipitation was performed to determine SUZ12 or H3K27me3 occupancy on the MEF2A promoter. Finally, the expression of human *Ahit* (LUNAR1) in the serum samples from patients of hypertrophic cardiomyopathy was tested by qRT-PCR.

**Results**—A previously unannotated lncRNA, *Ahit* (anti-hypertrophic interrelated transcript), was identified to be up-regulated in the mouse hearts after TAC. Inhibition of *Ahit* induced cardiac hypertrophy both *in vitro* and *in vivo*, associated with increased the expression of myocyte enhancer factor 2a (MEF2A), a critical transcriptional factor involved in cardiac hypertrophy. In

**Corresponding authors:** Chunyu Zeng, MD, PhD. chunyu.zeng01@163.com, Phone: (86)-02368757801; Fax: (86)-02368757801, Gengze Wu, MD, PhD. wugengze@163.com.

\*Contributed equally to this work

Disclosures  
None.

contrast, overexpression of *Ahit* significantly attenuated stress-induced cardiac hypertrophy *in vitro*. Furthermore, *Ahit* was significantly upregulated in serum samples of patients diagnosed with hypertensive heart disease versus non-hypertrophic hearts ( $1.46 \pm 0.17$  fold,  $p=0.0325$ ). Mechanistically, *Ahit* directly bound and recruited SUZ12, a core polycomb repressive complex 2 (PRC2) protein, to the promoter of MEF2A, triggering its trimethylation on H3 lysine 27 (H3K27me3) residues, and mediating the downregulation of MEF2A, thereby preventing cardiac hypertrophy.

**Conclusions**—*Ahit* is a lncRNA with a significant role in cardiac hypertrophy regulation through epigenomic modulation. *Ahit* is a potential therapeutic target of cardiac hypertrophy.

## Keywords

Cardiac hypertrophy; lncRNA; MEF2A; PRC2; SUZ12

---

Cardiac hypertrophy is an independent risk factor for the development of cardiovascular diseases, such as hypertension, acute myocardial infarction, arrhythmia, valvular heart disease, and heart failure. Cardiovascular disorders account for 13% of global mortality.<sup>1, 2</sup> However, the underlying molecular mechanisms of cardiac hypertrophy are still poorly understood. Discovery of new regulatory targets for cardiac hypertrophy is important for future therapeutic development to prevent and treat heart failure.

Although long non-coding RNAs (lncRNAs) generally do not encode proteins, they play important regulatory functions in all biological systems, including development, metabolism, and diseases.<sup>3–5</sup> The lncRNA mediated transcription regulations are extremely diverse and versatile, impacting on transcription by *cis*- and *trans*-activities, chromatin modifications, or regulating transcriptional factors translocation into or out of the nucleus.<sup>6–9</sup> More recent reports have demonstrated that lncRNAs play important roles in the regulation of cardiac hypertrophy. For example, lncRNA *Mhrt* can inhibit cardiac hypertrophy and prevents heart failure through BRG1;<sup>10</sup> on the other hand, lncRNA *Chast* is an inducer of cardiac hypertrophy;<sup>11</sup> lncRNA *CHRF* (cardiac hypertrophy related factor) induces cardiac hypertrophy by repressing miR-489 expression;<sup>12</sup> and H19 expression also negatively regulates cardiac hypertrophy.<sup>13</sup> Despite of these insights, global transcriptome analyses have identified thousands of lncRNAs that are potentially involved in cardiac hypertrophy. Yet, only a handful are well studied so far. Therefore, more studies are needed to identify and characterize functional lncRNAs in cardiac hypertrophy.

We identified a lncRNA 4833412C05Rik, named as *Ahit*, which was markedly up-regulated in the hypertrophic mouse hearts. *Ahit* was found to interact and recruit a chromatin modifier, PRC2 to the MEF2A promoter, leading to repressed expression of MEF2A and protected heart against cardiac hypertrophy under pathological stresses. Our results revealed a previously uncharacterized lncRNA that plays an anti-hypertrophic role in heart, and offered important new insights to the functional roles and therapeutic potential of cardiac lncRNAs in cardiac hypertrophy.

## Methods

Data and methods that are not directly available from this article are available from the corresponding authors upon reasonable request.

### Neonatal mouse, rat cardiomyocyte isolation, culture and treatment

Neonatal mouse (NMCM) or rat (NRCM) cardiomyocytes were obtained as previously described.<sup>14, 15</sup> Briefly, hearts were isolated from 1–3-day-old C57Bl/6J mice or Sprague–Dawley rats, washed and minced in Hank's balanced salt solution (HyClone, Waltham, MA). The minced neonatal hearts were dispersed by enzymatic digestion with 1.25 mg/mL trypsin (HyClone) and 0.8 mg/mL collagenase II (Worthington, Lakewood, NJ). After removing the fibroblasts by differential attachment for 90 min, the cardiomyocytes were plated in plates or slides according to the experimental need. The DMEM/F12 (Dulbecco's modified eagle medium) medium (Gibco, Grand Island, NY) contained 10% FBS (fetal bovine serum; Gibco), 100 U/ml penicillin/streptomycin, and 0.1 mM bromodeoxyuridine. After 18–24 hours, the cells were put into serum-free medium and transfected with siRNA (50 nM), using Lipofectamine RNAi MAX transfection reagent (Invitrogen, Carlsbad, CA). For *Ahit* overexpression, the sequence was synthesized and subcloned into pcDNA3.1 and transfected with Lipofectamine 3000 according to the manufacturer's protocol. The empty plasmid pcDNA3.1 was used as control. 24 hours later, the incubation media were removed and the cells treated with phenylephrine (PE, 10  $\mu$ M, Sigma, St. Louis, MO). After 48 hours treatment, the cells were harvested for RNA isolation or western blotting.

### Cultured cells other than cardiomyocyte

Primary cardiac fibroblasts (CFs) were obtained during the isolation of NMCMs based on different attaching time. CFs that attached to the dishes were cultured in DMEM/F12 medium (Gibco) supplemented with 10% FBS (Gibco). Two days later they were trypsinized and passaged at 1:3. This procedure yields cells that were almost fibroblasts by the first passage. Experiments were carried out after 2 or 3 passages.

Mouse C166 endothelial cell line (ECs), and mouse aortic vascular smooth muscle cell line (MOVAS), and human aortic smooth muscle cells (HASMCs) were purchased from ATCC and cultured at 37 °C in 95% O<sub>2</sub> and 5% CO<sub>2</sub> atmosphere in DMEM/F12 medium (Gibco) containing 10% FBS (Gibco).

### Microarray analysis

Total RNA was extracted from three mouse hearts 2 weeks after subjected to TAC and three mouse hearts from sham using Trizol reagent respectively. The microarray hybridization was performed based on the manufacturer's standard protocols by Shanghai Gminix Biological Information Company (Shanghai, China), using Affymetrix mouse lncRNA array. A random variance model (RVM) t-test was applied to discriminate differentially expressed mRNAs and lncRNAs between sham and TAC hearts. After false-discovery rate (FDR) analysis, the differential expressed lncRNAs were identified to have at least a 1.2-fold change  $p < 0.05$ , and  $q$ -value  $< 5\%$ .

### Human blood samples

All patients had signed written informed consents. This study was performed with the approval of the institutional ethical committee of The Third Military Medical University (Chongqing, China). Blood of patients diagnosed with hypertensive heart disease was centrifuged at 2000g for 10 min to obtain serum. Equivalent volume of serum was used to isolate RNA. The expression of human homologous *Ahit* was measured by qRT-PCR. Patient conditions are listed in the Supplementary Table 1.

### Western blotting

Western blotting was conducted to determine the protein level of MEF2A. Immunoblotting of 30 g protein was performed according to the manufacturer's instructions using rabbit anti-MEF2A antibody (Abcam, Cambridge, MA). The protein expression was normalized by GAPDH (Santa Cruz Biotechnology, Santa Cruz, CA).

### Quantitative RT-PCR

Total RNA from tissues or cells was extracted using Trizol reagent. One nanogram RNA was used to synthesize cDNA following the manufacturer's instructions (TAKARA, Kusatsu, Japan). Signal was detected by CFX96 Real-Time PCR Detection System (Bio-Rad, San Diego, CA), using SYBR Green dye (TAKARA). Target gene expressions were normalized by GAPDH mRNA. The PCR primers are listed in the Supplementary Table 2.

### Cell immunostaining

After fixing the cells with 4% paraformaldehyde for 20 minutes, they were permeabilized with 0.1% Triton X-100 for 10 minutes and blocked for 20 minutes. The NRCMs were treated with the indicated reagents and incubated with mouse anti- $\alpha$ -actinin (Sigma) overnight at 4°C. On the following day, the cells were incubated with Cy3-labeled goat anti-mouse IgG antibody (ZhongShanJinQiao, China). The nuclei were counterstained with DAPI. Images were acquired by Olympus AX70 laser confocal microscopy.

### Nuclear-cytoplasmic fractionation

Both nuclear and cytoplasmic RNA isolation from NMCMs were performed using the Cytoplasmic and Nuclear Protein Extraction Kit (Beyotime, China), following the manufacturer's instruction. Real-time PCR was used to detect the distribution of the target genes.

### RNA-FISH

Fluorescence *in Situ* Hybridization (FISH) Kit (Ribo, China) was performed, as in manufacturer's instructions. In brief, the NMCM, grown on slides, were fixed with 4% formaldehyde for 10 minutes at room temperature, followed by three washes with PBS (phosphate buffer saline) and 5 minutes of permeabilization with 0.5% Triton X-100. Then, the cells were washed with PBS thrice. Before hybridization, the cells were blocked with pre-hybridization buffer (Ribo), containing the blocking solution (99:1) at 37°C for 30 minutes. Then, 0.5 mM *Ahit* FISH probe was hybridized in hybridization buffer (Ribo) at 37°C overnight. After hybridization, the cells were washed with 4X sodium citrate buffer

(SSC) for 5 minutes thrice and 2X SSC, 1X SSC once at 42°C. The nuclei were stained with DAPI while NMCM microfilaments were stained with  $\alpha$ -actinin. After washing with PBS and sealing, photographs were taken by confocal microscopy. *Ahit* FISH probe was GGACATGTGTCCACAGTGTCCATACACCTTGCTC.

### Transverse Aortic Constriction

Transverse aortic constriction (TAC) was performed without intubation under anesthesia with isoflurane, as previously described.<sup>11–14</sup> All the use of mice for studies is in accordance with the regulations of the Third Military Medical University.

### RNA immunoprecipitation (RIP)

RIP experiments were performed to detect the interaction between RNA and protein using the Magna RIP™ RNA-Binding Protein Immunoprecipitation Kit (Millipore, Billerica, MA) in NMCMs. In brief,  $2 \times 10^7$  NMCMs were homogenized in lysis buffer that contained protease inhibitor cocktail and RNase inhibitor. The supernatant was centrifuged to remove the cell debris. At the same time, the protein A/G protein beads were incubated with SUZ12 antibody (Abcam) for 30 minutes. The beads/antibody complex and cell lysates were mixed in immunoprecipitation buffer and incubated overnight at 4°C. After the unbound protein was eluted and the enriched RNA was purified, SUZ12-associated RNA was detected by real-time PCR. Total RNA from the cell lysates was used as quality controls (Input), and normal mouse IgG was used as negative control.

### RNA pull-down assay

Biotinylated *Ahit* sense and antisense were transcribed using T7 RNA polymerase (Promega) and Biotin RNA Labeling Mix (Roche) *in vitro*, followed by purified with Quick Spin columns (Roche) according to the manufacturers' instructions. Three milligrams of biotinylated RNAs were degenerated at 65°C for 5 min in RNA structure buffer (10 mM MgCl<sub>2</sub>, 10 mM Tris-HCl, and 100 mM NH<sub>4</sub>Cl) and then let rest 20 min at room temperature. Freshly NMCMs were washed with ice-cold PBS and then treated with nuclear isolation buffer. Nuclear pellet was resuspended in RIPA buffer (150 mM KCl, 0.5 mM DTT, 25 mM Tris-HCl pH 7.4, 0.5% NP40), 1 mM PMSF (phenylmethylsulfonyl fluoride) and complete protease inhibitor cocktail (Roche). After mechanically sheared, nuclear membrane and debris were pelleted by centrifugation at 13,000×rpm for 10 min. Then the above processed RNA was mixed with the nuclear extract in RIPA buffer and incubated at room temperature for 1 hour. 50  $\mu$ L washed streptavidin agarose beads (Invitrogen) were added to each binding reaction and incubated at room temperature for 1.5 hour. The beads containing the RNA-protein complex were washed briefly thrice and then boiled in SDS-gel loading buffer. Retrieved proteins were detected by standard western blot technique.

### Chromatin immunoprecipitation (ChIP)

ChIP assays were performed using the EZ-CHIP Kit, according to the manufacturer's instructions (Millipore, 17–375). Briefly,  $1 \times 10^7$  cultured NMCMs with each treatment were washed and collected with ice-cold PBS containing protease inhibitor cocktail. Then, the precipitated cells were completely or partially digested by a moderate enzymatic cocktail

with non-crosslinking, obtaining chromatin fragments averaging one to a few nucleosomes in length. After diluting with ChIP dilution buffer, the digested chromatin was pre-cleared using protein A/G agarose beads and incubated with H3K27me3 (Abcam), SUZ12 (Abcam) antibodies, or normal mouse IgG at 4°C overnight. The following day, the antibody-chromatin complexes were recovered by incubation with protein A/G agarose beads at 4°C for 2 hours. After washing and purification, the immunoprecipitated DNA was analyzed by real-time PCR. Results were normalized to the input DNA, and normal mouse IgG was used as a negative control. The ChIP primer sequences are listed in the Supplementary Table 2.

### Administration of AAV9 vectors

To knockdown *Ahit* expression in the heart, mouse AAV9-sh*Ahit* constructs driven by cTnt (troponin T) promoter were synthesized and cloned by OBiO Technology Corp., Ltd (Shanghai, China). AAV9-empty was used as control.  $2 \times 10^{11}$  virus genome/mouse of control or AAV9-sh*Ahit* were injected into the abdominal cavity of neonatal C57Bl/6J mice. The expression of *Ahit* was detected one month after the injection. Sham or TAC surgeries were performed in infected mice at 2 months of age.

### Echocardiography

Echocardiography was performed one month after TAC or sham surgery. The mice were anesthetized using 1.5–2% isoflurane, keeping the heart rate at 450–550 beats/minute. Left ventricular internal dimensions at end-diastole and -systole (LVIDd and LVIDs) were measured under M-mode tracings from the short axis. Fractional shortening (FS, %) and ejection fraction (EF, %) were also calculated.

### Histological analysis

Hearts from all groups were fixed in 4% paraformaldehyde. Dehydration and embedding in paraffin used routine histological procedures. Subsequently, these samples were sectioned transversely at 5  $\mu$ m. The sections were stained with hematoxylin and eosin to determine the size and thickness of the heart wall or Masson's stain to evaluate the degree of fibrosis. The cardiomyocyte cross sectional area was assessed using FITC-conjugated wheat germ agglutinin (Invitrogen)-stained sections.

### Statistical analysis

Data are shown as mean $\pm$ SEM. Normality of data was tested with Shapiro-Wilk test using SPSS before statistical analysis. Student's t-test was used to compare two groups, and one-way ANOVA, followed by Holm-Sidak test, was used to compare more than two groups. Mann Whitney test was used to compare two groups of data without normality. All statistical analyses were performed with SPSS software. Statistical significance was set at  $P < 0.05$ .

## Results

### Identification of *Ahit* in response to hypertrophic stimulation *in vitro* and *in vivo*

To discover important lncRNAs associated with cardiac hypertrophy, a microarray (Affimatrix, see Methods) based expression analysis was performed using total RNA



isolated from pressure-overloaded mouse hearts induced by trans-aortic constriction (TAC) for 2 weeks. From three biological replicates each from the TAC and sham operated controls, 115 and 124 ncRNAs were found to be significantly up- or down-regulated respectively, with a fold-change  $>1.2$ ,  $P < 0.05$ , and false discovery rate  $< 0.05$  (Figure 1A) compared to the Sham hearts. Five lncRNAs were detected among the top 20 up-regulated ncRNAs based on fold of induction (Figure 1B and Supplementary Table 3), and the remaining 15 transcripts were either microRNAs or small nucleolar RNAs. Consistent with the microarray data, the upregulation of all the 5 lncRNAs, was validated by PCR, with Gm13054 ( $2.40 \pm 0.098$  fold,  $p < 0.0001$ ) and 4833412C05Rik ( $2.77 \pm 0.15$  fold,  $p = 0.0018$ ) showing the highest levels of induction (Figure 1C). Because Gm13054 is an antisense lncRNA while 4833412C05Rik is a long intergenic ncRNA, we focused on 4833412C05Rik, which was highly enriched in the heart, relative to the other organs (Figure 1C and 1D). To take into account the function of 4833412C05Rik (see below), we named it “*Ahit* (Anti-hypertrophic interrelated transcript)”.

*Ahit* is 1083 nucleotide long, containing three exons, and is significantly conserved in sequence and genome locus across multiple species (Figures 1E and 1F). Sequence evaluation using a Protein Coding Potential Calculator ([http://cpc.cbi.pku.edu.cn/programs/run\\_cpc.jsp](http://cpc.cbi.pku.edu.cn/programs/run_cpc.jsp)) detected low coding capacity for *Ahit*, like many well-established lncRNAs relative to the known coding genes (Figure 1G). We evaluated the time-course of *Ahit* expression following TAC in mouse hearts, and found *Ahit* was up-regulated at 2 weeks ( $1.83 \pm 0.15$  fold,  $p = 0.0108$ ) after left ventricular (LV) pressure overload which was sustained 10 weeks ( $2.10 \pm 0.23$  fold,  $p = 0.0182$ ) in mice, with a peak expression level detected at 6 weeks ( $4.48 \pm 0.58$  fold,  $p = 0.0365$ ) compared with sham hearts, suggesting *Ahit* might work in the entire process of cardiac remodeling (Figure 1H). Interestingly, another 850 nt lncRNA we named as *Ahit-V* (4833412C05Rik-202), was identified on the same chromosome locus as *Ahit* (Figure 1I). However, the expression of *Ahit* was significantly higher than *Ahit-V* variant in the mouse hearts at basal ( $0.54 \pm 0.11$  fold versus *Ahit*,  $p = 0.0113$ ) (Figure 1J). Moreover, *Ahit* but not *Ahit-V* was induced in post-TAC hearts, indicating that *Ahit* ( $2.775 \pm 0.15$  fold,  $p = 0.0018$ ), not *Ahit-V* ( $1.292 \pm 0.04$  fold,  $p = 0.2366$ ), is more likely related to cardiac hypertrophy. (Figure 1K). *Ahit* expression in cardiac fibroblasts, endothelial cells, and mouse aortic vascular smooth muscle cells were detected but at much lower levels than in cardiomyocytes (Supplementary Figure 1). In cultured neonatal rat cardiomyocytes (NRCMs), hypertrophic stimulation by phenylephrine (PE, 10  $\mu$ M, 48 h) treatment<sup>16</sup> significantly induced *Ahit* expression ( $2.21 \pm 0.02$  fold,  $p = 0.0002$ ) (Figure 1L), further indicating its potential function in hypertrophy.

### ***Ahit* suppresses PE induced cardiomyocyte hypertrophy *in vitro***

Based on the observation that *Ahit* was up-regulated by hypertrophic stimuli, we next studied the consequences of loss-of-*Ahit* expression in NRCMs (NRCMs were not used because they do not hypertrophy in response to PE, data not shown). Using siRNA designed from the conserved region in both rat and mouse *Ahit* transcript, *Ahit* expression was significantly reduced in NRVM ( $0.52 \pm 0.04$  fold versus scramble,  $p = 0.0017$ ) (Figure 2A), while *Ahit-V* expression was not affected ( $0.88 \pm 0.03$  fold versus scramble,  $p = 0.1802$ ) (Supplementary Figure 2). *Ahit* inhibition showed no impact on myocyte sizes (based on  $\alpha$ -

actinin-positive staining) or the expression of hypertrophic markers, including ANP, BNP or  $\beta$ -MHC (Supplementary Figure 3). However, cardiomyocytes sizes were significantly more enlarged in the *Ahit*-knockdown myocytes following PE treatment (PE versus scramble 1.33 $\pm$ 0.02 fold,  $p=0.0011$ , si*Ahit*+PE versus PE 1.59 $\pm$ 0.04 fold,  $p=0.0036$ ) (Figures 2B and 2C). In addition, the expressions of cardiac hypertrophy markers, including ANP, BNP, and  $\beta$ -MHC were further augmented (Figure 2D). In contrast, overexpression of *Ahit* attenuated PE-induced cardiac hypertrophy, as measured from both cell sizes and the expressions of hypertrophic marker genes, ANP, BNP, and  $\beta$ -MHC were inhibited (Figures 3A–3D). These results suggest that *Ahit* is a potent negative regulator of cardiac hypertrophy.

### Down-regulation of *Ahit* promotes cardiac hypertrophy in vivo

To determine if *Ahit* has an anti-hypertrophic effect *in vivo*, neonatal mice (1–3 days after birth) were infected with a single intraperitoneal injection of AAV9-sh*Ahit* under the control of the cardiac troponin T promoter ( $2 \times 10^{11}$  virus genome per mouse) (Figure 4A). An empty vector (AAV9-empty) without the *Ahit* sequence was used as a control. Treatment of AAV9-shRNA decreased the cardiac *Ahit* expression by 43% (versus AAV9-empty,  $p=0.0002$ ) (Figure 4B). In either AAV treated groups, the mice showed no anatomical or functional abnormalities in heart at baseline (Supplementary Figure 5A,5B,5C,5D,5E,5F). Pressure-overload was induced by TAC at 2 month of age. In the AAV9-empty treated mice, the expression of *Ahit* was induced more than two folds after TAC, in contrast to approximately 1.2 folds in the AAV9-sh*Ahit* treated hearts (Supplementary Figure 4). At one month after TAC, the AAV9-sh*Ahit* treated mice exhibited a significantly more severe hypertrophy and cardiac dysfunction, relative to the mice treated with AAV9-empty (Figures 4C–4K). This was manifested in a significant lower systolic function, as measured by the decrease in the percent ejection fraction (EF) (TAC versus sham 0.86 $\pm$ 0.04 fold,  $p=0.026$ , TAC+sh*Ahit* versus TAC 0.81 $\pm$ 0.07 fold,  $p=0.0796$ ) and fractional shortening (FS) (TAC versus sham 0.81 $\pm$ 0.05 fold,  $p=0.0269$ , TAC+sh*Ahit* versus TAC 0.72 $\pm$ 0.08 fold,  $p=0.0373$ ) and higher chamber dilation, as measured in diastolic (LVIDd) (TAC versus sham 1.24 $\pm$ 0.06 fold,  $p=0.0512$ , TAC+sh*Ahit* versus TAC 1.29 $\pm$ 0.07 fold,  $p=0.0063$ ) and systolic ventricular internal diameters (LVIDs) (TAC versus sham 1.45 $\pm$ 0.11 fold,  $p=0.0163$ , TAC+sh*Ahit* versus TAC 1.51 $\pm$ 0.13 fold,  $p=0.0086$ ) (Figures 4C–4F). These findings were corroborated by higher levels of the heart weight versus body weight ratio (TAC versus sham 1.32 $\pm$ 0.03 fold,  $p<0.0001$ , TAC+sh*Ahit* versus TAC 1.17 $\pm$ 0.01 fold,  $p=0.0002$ ), bigger chamber size, cross-section areas and cardiomyocyte size (TAC versus sham 1.28 $\pm$ 0.07 fold,  $p=0.0481$ , TAC+sh*Ahit* versus TAC 1.16 $\pm$ 0.02 fold,  $p=0.0395$ ) (Figures 4G–4J and 4L). In addition, the degree of cardiac fibrosis was greater in the *Ahit* down-regulated mice than in the controls (TAC versus sham 2.28 $\pm$ 0.24 fold,  $p=0.0018$ , TAC+sh*Ahit* versus TAC 1.64 $\pm$ 0.25 fold,  $p=0.042$ ) (Figure 4K and 4M). Collectively, these data show that *Ahit* deficiency aggravates the pathological cardiac hypertrophy and dysfunction in heart caused by TAC, supporting an anti-hypertrophy role for *Ahit in vivo*.

### Anti-hypertrophy role of *Ahit* is via *in cis* regulation of MEF2A expression

A well-known function of lncRNA is *cis*-or *trans*- regulation of either neighboring genes or global transcriptome. One of the neighboring genes of *Ahit* (Chromosome 7: 67,784,538–67,804,139 reverse strand) is myocyte enhancer factor 2A (MEF2A) (Chromosome 7:



67,231,163–67,372,858 reverse strand), which is a well-studied transcriptional factor for cardiac genes (Figure 5A). Down-regulation of *Ahit* expression by siRNA ( $0.26\pm 0.02$  fold versus scramble,  $p=0.0008$ ) increased both the mRNA ( $2.78\pm 0.51$  fold versus scramble,  $p=0.01$ ) and the protein expressions ( $2.31\pm 0.04$  fold versus scramble,  $p<0.0001$ ) of MEF2A in NCMs (Figures 5B–5D). These results were corroborated *in vivo*; silencing *Ahit* with AAV9 shRNA in mouse heart increased the MEF2A expression ( $2.26\pm 0.34$  fold versus AAV9-empty,  $p=0.0058$ ) (Figure 5E). To show the further role of MEF2A in the *Ahit*-mediated cardiac hypertrophy regulation, we treated NRCM with both siRNAs against *Ahit* and MEF2A simultaneously followed by PE stimulation. Consistent with the previous results, *Ahit* knockdown enlarged the NRCM cell size and increased the expressions of cardiac hypertrophy-related genes, ANP, BNP, and  $\beta$ -MHC. In contrast, co-treatment of *Ahit* siRNA with MEF2A siRNA effectively abrogated the *Ahit* siRNA-mediated effects (Figures 5F–5I). Therefore, *Ahit*-mediated inhibition of cardiac hypertrophy involves downstream regulation of MEF2A expression.

MEF2 family comprised of four homologous genes, including MEF2A, MEF2B, MEF2C, and MEF2D. Apart from MEF2A, we also assessed the other three family members after *Ahit* knockdown *in vivo* and *in vitro*. Although all MEF2 members were further induced after *Ahit* down-regulated, the induction of MEF2A ( $2.78\pm 0.51$  fold versus scramble,  $p=0.01$ ) had the highest fold change. (Supplementary Figure 6).

### ***Ahit* is a nuclear lncRNA and interacts with SUZ12 directly to regulate PRC2 occupancy on the MEF2A promoter and modulates histone modification**

To explore the molecular mechanism by which *Ahit* negatively regulates MEF2A expression, we first performed RNA fluorescence *in situ* hybridization (FISH) to determine the cellular localization of *Ahit*. The result showed that *Ahit* was mainly located in the nucleus (Figure 6A). Using small nucleolar snoRNA and the Nuclear-Enriched Abundant Transcript 1 (NEAT1) lncRNA as benchmark controls in nuclear/cytoplasmic RNA fractionation assay, we also found *Ahit* was mainly a nucleus-localized lncRNA (Figure 6B).

Previous studies have suggested that nuclear localized lncRNAs often interact with various nuclear proteins to exert its gene regulatory function through epigenetic modulation by recruiting histone modifying complexes such as PRC2<sup>17</sup>. Using an online tool, catRAPID ([http://s.tartagialab.com/page/catrapid\\_group](http://s.tartagialab.com/page/catrapid_group)), we screened potential proteins that may interact with *Ahit*, and identified SUZ12, a core member of PRC2 complex, has a high probability to directly interact with *Ahit* (Figure 6C). RNA immunoprecipitation (RIP) with an anti-SUZ12 antibody, the endogenous *Ahit* was detected with 24.86-fold enrichment vs. IgG control (Figure 6D), significantly higher than other components of PRC2 (Supplementary Figure 7). Reversely, using RNA pulldown of *Ahit* associated proteins, we detected SUZ12 (Figure 6E). PRC2 catalyzes trimethylation of histone H3 on lysine 27 (H3K27me3), which represses local nucleosomes from active transcription<sup>18</sup>. Chromatin immunoprecipitation (ChIP) was performed in NCMs using anti-SUZ12 antibody. We designed five primers covering 1500 base-pairs of the MEF2A proximal promoter region. After silencing *Ahit*, the occupancy of PRC2 on the MEF2A promoter was decreased relative to control (scramble siRNA) (Figure 7A). Figure 7B showed that there was a decline

of H3K27me3 levels on the MEF2A promoter when *Ahit* was silenced in NCMCs. Therefore, H3K27me3 modification on the MEF2A promoter is affected by *Ahit* expression. Indeed, using an on-line program called LongTarget to calculate the probability of direct interaction between RNA and DNA (<http://lncrna.smu.edu.cn/show/DNATriplex>), we find *Ahit* and MEF2A promoter has significant potential interaction. The result showed that the interaction between *Ahit* and MEF2A promoter was significant. The triplex-forming oligonucleotides (TFOs) of *Ahit* and triplex target sites (TTSs) of MEF2A promoter were presented in Supplementary Table 4. Also, we compared the evolutionary conservation of the MEF2A promoter regions between human and mouse, and found a sequence identity of 54% (Supplementary Figure 8).

### ***Ahit* expression is correlated with cardiac hypertrophy in human**

The human homolog of *Ahit* was identified as lncRNA LUNAR1 based on conserved genomic localization and its close distance to the human MEF2A gene. Using human smooth muscle cells as in vitro system, we found LUNAR1 knockdown significantly upregulated human MEF2A expression 1.57±0.11 fold versus scramble, p=0.023) (Figure 8A). Next, we used qRT-PCR to detect the expression of LUNAR1 in the serum of a cohort of patients diagnosed with hypertensive heart disease and found LUNAR1 was upregulated in the patient samples compared to the healthy controls (1.46±0.17 fold, p=0.022) (Figure 8B). Therefore, the expression of human homolog of *Ahit*, LUNAR1, may also be correlated with the development of cardiac hypertrophy.

## **Discussion**

lncRNAs account for the majority of ncRNAs that are previously thought to be transcription byproducts of RNA polymerase II and do not have major biological functions.<sup>19</sup> However, recent studies have shown that lncRNAs interact with DNAs, transcription factors, and RNA binding proteins; and they regulate a variety of biological processes.<sup>20, 21</sup> Some lncRNAs have been shown to be closely associated with cardiac development and progression of cardiovascular diseases. The lncRNA Braveheart plays an important role in the establishment of cardiovascular lineage;<sup>22</sup> Fendrr is an essential regulatory factor for mouse heart and body wall development;<sup>23</sup> ANRIL expression is associated with the severity of atherosclerosis;<sup>24</sup> and lincRNA-P21 is important in the regulation of neointima formation, vascular smooth muscle cell proliferation, and apoptosis.<sup>25</sup> Although there are many studies related to lncRNA in the cardiovascular field, there are not as many studies on the role of lncRNA in the regulation of cardiac hypertrophy. In this report, we identified a new and functional lncRNA *Ahit* as a potent regulator of cardiac hypertrophy.

Over the past decades, genetically modified animal models of cardiac hypertrophy have identified numerous pathways or genes, but the progress is limited.<sup>26, 27</sup> Most of the well-known molecules related to cardiac hypertrophy are coding genes, which compose less than 2% of the genome. By contrast, there are only a few of reports on the role of lncRNAs on cardiac hypertrophy. For example, the repression of the lncRNA Mhrt by Brg1, a histone acetylation factor, induced cardiac hypertrophy.<sup>10</sup> *Chast* was discovered from the microarray of TAC-induced cardiac hypertrophy to promote cardiac remodeling.<sup>11</sup> *Chaer* was found to

be dysregulated in pressure-overload-induced mouse failing heart, and negatively regulated PRC2 action on H3K27me3 expression.<sup>28</sup> CHRFB was found to inhibit miR-489 and promote cardiac hypertrophy caused by angiotensin II treatment in mice.<sup>12</sup> Although these lncRNAs are important in cardiac remodeling, there are still many more lncRNAs to be studied in the context of cardiac hypertrophy and remodeling. Consistent with most reports, we used microarray to analyze the transcriptome of the heart at two-week time point after TAC, when cardiac remodeling may begin.<sup>29–32</sup> *Ahit* is a cardiac-enriched lncRNA. It is more abundantly expressed in the heart than other tissues and its expression is closely related to cardiac hypertrophy. *Ahit* is upregulated by pressure overload *in vivo* as well as the *in vitro* model of cardiomyocyte hypertrophy caused by PE. This phenotype is consistent with our finding that down-regulation of *Ahit* promotes cardiac hypertrophy *in vitro* and *in vivo*.

*Ahit* is a neighboring gene of MEF2A, which is a critical regulator of cardiac development and cardiac gene expression and is expressed in many tissues, including the myocardium.<sup>33, 34</sup> MEF2A belongs to the MEF2 family comprised of four homologous genes, including MEF2B, MEF2C, and MEF2D.<sup>35</sup> MEF2 can activate the expression of fetal genes, such as ANP and can regulate other core cardiac transcriptional factors, such as GATA and NKX.<sup>36–38</sup> Cardiac-specific over-expression of MEF2A or MEF2C in transgenic mice causes myocardial hypertrophy.<sup>39</sup> Consistent with these findings, silencing of *Ahit* increases the expression of MEF2 family *in vitro* and *in vivo*, with the change of MEF2A expression to be the most significant. This is also consistent with exacerbated pathological cardiac hypertrophy in the *Ahit* knockdown hearts, as evidenced by the increase in cardiomyocyte surface area and cardiac stress markers. Whether *Ahit* regulates MEF2A expression by *cis*-mechanism or *trans*-regulation, and whether its effects on other MEF2 gene family members a direct action or indirect, remain to be further studied.

Unlike miRNAs, which often inhibit gene expression, lncRNAs can activate or inhibit gene expression.<sup>8, 40</sup> Our data showed that *Ahit* was predominantly located in the nucleus, where it regulates gene expression at the epigenetic level. Many studies have revealed that many lncRNAs are predominantly in the nucleus and can be in direct contact with target genes to form RNA-DNA-protein complexes or recruit nuclear proteins to modify the chromatin, triggering chromatin conformation changes.<sup>6,9,17,41</sup> Through online bioinformatic prediction, we find *Ahit* has the potential to interact with multiple subunits of PRC2 complex, including SUZ12, EED (embryonic ectoderm development) and EZH2 (enhancer of zeste homolog 2). But RIP and RNA pulldown experiments indicated, compared with EED and EZH2, the binding capacity between SUZ12 and *Ahit* has the highest binding activity. SUZ12 is a core component of PRC2 that catalyzes the trimethylation of histone H3K27 (H3K27me3), thereby leading to the “closing” of chromatin structure, and silencing of gene expression.<sup>42–44</sup> The lncRNA-mediated recruitment of PRC2 to the promoter of target genes triggers the tri-methylation of H3 lysine 27, H3K27me3.<sup>45–47</sup> Our data shows *Ahit* can modulate PRC2-MEF2A promoter interaction, possibly through RNA-DNA interaction. Previous studies have shown that PRC2 can induce cell proliferation<sup>42,46</sup> and cardiac hypertrophy.<sup>28</sup> In our study, decreasing *Ahit* abundance through siRNA decreases the level of H3K27me3 and PRC2 occupancy to the MEF2A promoter, in association with

its activation during hypertrophy. As aforementioned, lncRNAs play important roles in cardiac development and related diseases<sup>10–13,22–25</sup> by interacting with PRC2<sup>17, 18, 28, 42–47</sup>.

It is generally known that the conservations of lncRNAs are lower than mRNAs<sup>8, 40</sup>. However in our study, we found lncRNA LUNAR1 was the homologous gene of *Ahit* in human. The sequence identity between them is 33% likely due to difference in lengths, LUNAR1 is 2516 bp, and *Ahit* is 1096 bp. However, the gene locus of LUNAR1 in human genome is conserved to *Ahit* in mouse genome, including their close distance with MEF2A. What's more, LUNAR1 can regulate the expression of MEF2A in human cell. When LUNAR1 was downregulated, MEF2A was increased, indicating a functional conservation of *Ahit* homologous gene in human. Moreover, we found the expression of LUNAR1 was higher in serum of patients with cardiac hypertrophy. This is an interesting finding because it indicates that *Ahit* has the potential to translate into clinical for diagnosis and treatment of cardiomyopathy.

In summary, our present work reveals a previously uncharacterized lncRNA, *Ahit* that acts as an anti-hypertrophic regulator. *Ahit* protects against cardiac hypertrophy by modulating chromatin remodeling via direct binding with SUZ12, and recruiting PRC2 to promote trimethylation of H3K27 on the MEF2A promoter region. Finally, expression of *Ahit* inhibits transcription factor MEF2A expression to prevent the activation of cardiac hypertrophy-related genes, blocking cardiac remodeling (Figure 9). These discoveries provide new insights into the mechanism of cardiac hypertrophy and have important implications for the diagnosis and treatment of pathological cardiac hypertrophy by targeting lncRNA.

## Supplementary Material

Refer to Web version on PubMed Central for supplementary material.

## Acknowledgments

### Sources of Funding

These studies were supported in part by grants from the National Key R&D Program of China (2018YFC1312700), the National Natural Science Foundation of China (31600936, 81930008), Program of Innovative Research Team by National Natural Science Foundation (81721001), and the National Institutes of Health (5R01DK039308-31, 7R37HL023081-37, 5P01HL074940-11).

## Non-standard Abbreviations and Acronyms

<b>AAV9</b>	Adeno- associated virus, serotype 9
<b>Ahit</b>	Anti-hypertrophic interrelated transcript
<b>ANP</b>	Atrial natriuretic peptide
<b>BNP</b>	Brain natriuretic peptide
<b>CFs</b>	Cardiac fibroblasts
<b>ChIP</b>	Chromatin immunoprecipitation

<b>ECs</b>	Endothelial cells
<b>EF</b>	Ejection fraction
<b>FS</b>	Fractional shortening
<b>LUNAR1</b>	Leukemia-associated non-coding IGF1R activator RNA 1
<b>MEF2A</b>	Myocyte enhancer factor 2A
<b>ncRNA</b>	Non-coding RNA
<b>NMCM</b>	Neonatal mouse cardiomyocytes
<b>NRCM</b>	Neonatal rat cardiomyocytes
<b>PBS</b>	Phosphate buffer saline
<b>PE</b>	Phenylephrine
<b>PRC2</b>	Polycomb repressive complex 2
<b>qRT-PCR</b>	Quantitative real-time polymerase chain reaction
<b>RIP</b>	RNA immunoprecipitation
<b>SUZ12</b>	Suppressor of zeste 12 protein homolog
<b>TAC</b>	Transverse aortic constriction
<b>β-MHC</b>	Myosin heavy chain beta isoform

## References

1. Frey N, Katus HA, Olson EN, Hill JA. Hypertrophy of the heart: A new therapeutic target? *Circulation*. 2004;109:1580–1589 [PubMed: 15066961]
2. Dezsi CA. Differences in the clinical effects of angiotensin-converting enzyme inhibitors and angiotensin receptor blockers: A critical review of the evidence. *Am J Cardiovasc Drugs*. 2014;14:167–173 [PubMed: 24385234]
3. Yin Y, Yan P, Lu J, Song G, Zhu Y, Li Z, Zhao Y, Shen B, Huang X, Zhu H, Orkin SH, Shen X. Opposing roles for the lncRNA Haunt and its genomic locus in regulating HOXA gene activation during embryonic stem cell differentiation. *Cell Stem Cell*. 2015;16:504–516 [PubMed: 25891907]
4. Thum T, Condorelli G. Long noncoding RNAs and microRNAs in cardiovascular pathophysiology. *Circ Res*. 2015;116:751–762 [PubMed: 25677521]
5. Batista PJ, Chang HY. Long noncoding RNAs: Cellular address codes in development and disease. *Cell*. 2013;152:1298–1307 [PubMed: 23498938]
6. Wang KC, Chang HY. Molecular mechanisms of long noncoding RNAs. *Mol Cell*. 2011;43:904–914 [PubMed: 21925379]
7. Yan P, Luo S, Lu JY, Shen X. Cis- and trans-acting lncRNAs in pluripotency and reprogramming. *Curr Opin Genet Dev*. 2017;46:170–178 [PubMed: 28843809]
8. Devaux Y, Zangrando J, Schroen B, Creemers EE, Pedrazzini T, Chang CP, Dorn GW, 2nd, Thum T, Heymans S. Long noncoding RNAs in cardiac development and ageing. *Nat Rev Cardiol*. 2015;12:415–425 [PubMed: 25855606]
9. Li T, Mo X, Fu L, Xiao B, Guo J. Molecular mechanisms of long noncoding RNAs on gastric cancer. *Oncotarget*. 2016;7:8601–8612 [PubMed: 26788991]

10. Han P, Li W, Lin CH, Yang J, Shang C, Nuernberg ST, Jin KK, Xu W, Lin CY, Lin CJ, Xiong Y, Chien H, Zhou B, Ashley E, Bernstein D, Chen PS, Chen HV, Quertermous T, Chang CP. A long noncoding RNA protects the heart from pathological hypertrophy. *Nature*. 2014;514:102–106 [PubMed: 25119045]
11. Viereck J, Kumarswamy R, Foinquinos A, Xiao K, Avramopoulos P, Kunz M, Dittrich M, Maetzig T, Zimmer K, Remke J, Just A, Fendrich J, Scherf K, Bolesani E, Schambach A, Weidemann F, Zweigerdt R, de Windt LJ, Engelhardt S, Dandekar T, Batkai S, Thum T. Long noncoding RNA *Chast* promotes cardiac remodeling. *Sci Transl Med*. 2016;8:326ra322
12. Wang K, Liu F, Zhou LY, Long B, Yuan SM, Wang Y, Liu CY, Sun T, Zhang XJ, Li PF. The long noncoding RNA *CHRF* regulates cardiac hypertrophy by targeting miR-489. *Circ Res*. 2014;114:1377–1388 [PubMed: 24557880]
13. Liu LT, An XB, Li ZH, Song Y, Li LL, Zuo S, Liu N, Yang G, Wang HJ, Cheng X, Zhang YY, Yang X, Wang J. The H19 long noncoding RNA is a novel negative regulator of cardiomyocyte hypertrophy. *Cardiovasc Res*. 2016;111:56–65 [PubMed: 27084844]
14. Seok HY, Chen J, Kataoka M, Huang ZP, Ding J, Yan J, Hu X, Wang DZ. Loss of microRNA-155 protects the heart from pathological cardiac hypertrophy. *Circ Res*. 2014;114:1585–1595 [PubMed: 24657879]
15. Jiang DS, Wei X, Zhang XF, Liu Y, Zhang Y, Chen K, Gao L, Zhou H, Zhu XH, Liu PP, Bon Lau W, Ma X, Zou Y, Zhang XD, Fan GC, Li H. IRF8 suppresses pathological cardiac remodelling by inhibiting calcineurin signalling. *Nat Commun*. 2014;5:3303 [PubMed: 24526256]
16. Wei X, Wu B, Zhao J, Zeng Z, Xuan W, Cao S, Huang X, Asakura M, Xu D, Bin J, Kitakaze M, Liao Y. Myocardial Hypertrophic Preconditioning Attenuates Cardiomyocyte Hypertrophy and Slows Progression to Heart Failure Through Upregulation of S100A8/A9. *Circulation*. 2015;131:1506–1517. [PubMed: 25820336]
17. Quinodoz S, Guttman M. Long noncoding RNAs: an emerging link between gene regulation and nuclear organization. *Trends Cell Biol*. 2014;24:651–663 [PubMed: 25441720]
18. Yoo KH, Hennighausen L. EZH2 methyltransferase and H3K27 methylation in breast cancer. *Int J Biol Sci*. 2012;8:59–65 [PubMed: 22211105]
19. Comings DE. The structure and function of chromatin. *Adv Hum Genet*. 1972;3:237–431 [PubMed: 4578264]
20. Mattick JS. The genetic signatures of noncoding RNAs. *PLoS Genet*. 2009;5:e1000459 [PubMed: 19390609]
21. Mattick JS, Amaral PP, Dinger ME, Mercer TR, Mehler MF. RNA regulation of epigenetic processes. *Bioessays*. 2009;31:51–59 [PubMed: 19154003]
22. Klattenhoff CA, Scheuermann JC, Surface LE, Bradley RK, Fields PA, Steinhilber ML, Ding H, Butty VL, Torrey L, Haas S, Abo R, Tabebordbar M, Lee RT, Burge CB, Boyer LA. Braveheart, a long noncoding RNA required for cardiovascular lineage commitment. *Cell*. 2013;152:570–583 [PubMed: 23352431]
23. Grote P, Wittler L, Hendrix D, Koch F, Wahrlich S, Beisaw A, Macura K, Blass G, Kellis M, Werber M, Herrmann BG. The tissue-specific lncRNA *Fendrr* is an essential regulator of heart and body wall development in the mouse. *Dev Cell*. 2013;24:206–214 [PubMed: 23369715]
24. Holdt LM, Beutner F, Scholz M, Gielen S, Gabel G, Bergert H, Schuler G, Thiery J, Teupser D. ANRIL expression is associated with atherosclerosis risk at chromosome 9p21. *Arterioscler Thromb Vasc Biol*. 2010;30:620–627 [PubMed: 20056914]
25. Wu G, Cai J, Han Y, Chen J, Huang ZP, Chen C, Cai Y, Huang H, Yang Y, Liu Y, Xu Z, He D, Zhang X, Hu X, Pinello L, Zhong D, He F, Yuan GC, Wang DZ, Zeng C. LincRNA-p21 regulates neointima formation, vascular smooth muscle cell proliferation, apoptosis, and atherosclerosis by enhancing p53 activity. *Circulation*. 2014;130:1452–1465 [PubMed: 25156994]
26. Heineke J, Molkenin JD. Regulation of cardiac hypertrophy by intracellular signalling pathways. *Nat Rev Mol Cell Biol*. 2006;7:589–600 [PubMed: 16936699]
27. Molkenin JD, Robbins J. With great power comes great responsibility: Using mouse genetics to study cardiac hypertrophy and failure. *J Mol Cell Cardiol*. 2009;46:130–136 [PubMed: 18845155]
28. Wang Z, Zhang XJ, Ji YX, Zhang P, Deng KQ, Gong J, Ren S, Wang X, Chen I, Wang H, Gao C, Yokota T, Ang YS, Li S, Cass A, Vondriska TM, Li G, Deb A, Srivastava D, Yang HT, Xiao X, Li



- H, Wang Y. The long noncoding RNA *Chaer* defines an epigenetic checkpoint in cardiac hypertrophy. *Nat Med*. 2016;22:1131–1139 [PubMed: 27618650]
29. Traynham CJ, Cannavo A, Zhou Y, Vouga AG, Woodall BP, Hullmann J, Ibetti J, Gold JJ, Chuprun JK, Gao E, Koch WJ. Differential role of G protein-coupled receptor kinase 5 in physiological versus pathological cardiac hypertrophy. *Circ Res*. 2015;117:1001–1012 [PubMed: 26515328]
  30. Matsushima S, Kuroda J, Zhai P, Liu T, Ikeda S, Nagarajan N, Oka S, Yokota T, Kinugawa S, Hsu CP, Li H, Tsutsui H, Sadoshima J. Tyrosine kinase FYN negatively regulates NOX4 in cardiac remodeling. *J Clin Invest*. 2016;126:3403–3416 [PubMed: 27525436]
  31. Shirakabe A, Zhai P, Ikeda Y, Saito T, Maejima Y, Hsu CP, Nomura M, Egashira K, Levine B, Sadoshima J. Drp1-dependent mitochondrial autophagy plays a protective role against pressure overload-induced mitochondrial dysfunction and heart failure. *Circulation*. 2016;133:1249–1263 [PubMed: 26915633]
  32. Witt H, Schubert C, Jaekel J, Fliegner D, Penkalla A, Tiemann K, Stypmann J, Roepcke S, Brokat S, Mahmoodzadeh S, Brozova E, Davidson MM, Ruiz Noppinger P, Grohe C, Regitz-Zagrosek V. Sex-specific pathways in early cardiac response to pressure overload in mice. *J Mol Med (Berl)*. 2008;86:1013–1024 [PubMed: 18665344]
  33. McCalmon SA, Desjardins DM, Ahmad S, Davidoff KS, Snyder CM, Sato K, Ohashi K, Kielbasa OM, Mathew M, Ewen EP, Walsh K, Gavras H, Naya FJ. Modulation of angiotensin II-mediated cardiac remodeling by the MEF2A target gene Xirp2. *Circ Res*. 2010;106:952–960 [PubMed: 20093629]
  34. Kain V, Kapadia B, Viswakarma N, Seshadri S, Prajapati B, Jena PK, Teja Meda CL, Subramanian M, Kaimal Suraj S, Kumar ST, Prakash Babu P, Thimmapaya B, Reddy JK, Parsa KV, Misra P. Co-activator binding protein PIMT mediates TNF- $\alpha$  induced insulin resistance in skeletal muscle via the transcriptional down-regulation of MEF2A and GLUT4. *Sci Rep*. 2015;5:15197 [PubMed: 26468734]
  35. Liu N, Nelson BR, Bezprozvannaya S, Shelton JM, Richardson JA, Bassel-Duby R, Olson EN. Requirement of MEF2A, C, and D for skeletal muscle regeneration. *Proc Natl Acad Sci U S A*. 2014;111:4109–4114 [PubMed: 24591619]
  36. Bar H, Kreuzer J, Cojoc A, Jahn L. Upregulation of embryonic transcription factors in right ventricular hypertrophy. *Basic Res Cardiol*. 2003;98:285–294 [PubMed: 12955401]
  37. Potthoff MJ, Olson EN. MEF2: A central regulator of diverse developmental programs. *Development*. 2007;134:4131–4140 [PubMed: 17959722]
  38. Karamboulas C, Dakubo GD, Liu J, De Repentigny Y, Yutzey K, Wallace VA, Kothary R, Skerjanc IS. Disruption of MEF2 activity in cardiomyoblasts inhibits cardiomyogenesis. *J Cell Sci*. 2006;119:4315–4321 [PubMed: 17003108]
  39. Xu J, Gong NL, Bodi I, Aronow BJ, Backx PH, Molkenin JD. Myocyte enhancer factors 2A and 2C induce dilated cardiomyopathy in transgenic mice. *J Biol Chem*. 2006;281:9152–9162 [PubMed: 16469744]
  40. Schonrock N, Harvey RP, Mattick JS. Long noncoding RNAs in cardiac development and pathophysiology. *Circ Res*. 2012;111:1349–1362 [PubMed: 23104877]
  41. Clemson CM, Hutchinson JN, Sara SA, Ensminger AW, Fox AH, Chess A, Lawrence JB. An architectural role for a nuclear noncoding RNA: Neat1 RNA is essential for the structure of paraspeckles. *Mol Cell*. 2009;33:717–726 [PubMed: 19217333]
  42. Margueron R, Reinberg D. The polycomb complex PRC2 and its mark in life. *Nature*. 2011;469:343–349 [PubMed: 21248841]
  43. Holoch D, Margueron R. Mechanisms regulating PRC2 recruitment and enzymatic activity. *Trends Biochem Sci*. 2017;42:531–542 [PubMed: 28483375]
  44. Beltran M, Yates CM, Skalska L, Dawson M, Reis FP, Viiri K, Fisher CL, Sibley CR, Foster BM, Bartke T, Uie J, Jenner RG. The interaction of PRC2 with RNA or chromatin is mutually antagonistic. *Genome Res*. 2016;26:896–907 [PubMed: 27197219]
  45. Khalil AM, Guttman M, Huarte M, Garber M, Raj A, Morales DR, Thomas K, Presser A, Bernstein BE, van Oudenaarden A, Regev A, Lander ES, Rinn JL. Many human large intergenic noncoding RNAs associate with chromatin-modifying complexes and affect gene expression. *Proc Natl Acad Sci USA*. 2009;106:11667–11672 [PubMed: 19571010]

46. Beckedorff FC, Ayupe AC, Crocci-Souza R, Amaral MS, Nakaya HI, Soltys DT, Menck CF, Reis EM, Verjovski-Almeida S. The intronic long noncoding RNA ANRASSF1 recruits PRC2 to the RASSF1A promoter, reducing the expression of RASSF1A and increasing cell proliferation. *PLoS Genet.* 2013;9:e1003705 [PubMed: 23990798]
47. Kim DH, Xi Y, Sung S. Modular function of long noncoding RNA, COLDAIR, in the vernalization response. *PLoS Genet.* 2017;13:e1006939 [PubMed: 28759577]

Author Manuscript

Author Manuscript

Author Manuscript

Author Manuscript

### Short Commentary

#### What is new?

- We identified a novel lncRNA anti-hypertrophic interrelated transcript (*Ahit*) to be upregulated during the pressure-overload induced mouse heart failure model.
- *Ahit* is an anti-hypertrophic regulator both in vivo and in vitro.
- *Ahit* serves as a scaffold to guide the SUZ12 to the promoter of MEF2A (a critical inducer of cardiac hypertrophy), leading to repressive H3K27me3 and decreased expression of MEF2A, thereby restricting cardiac hypertrophy.

#### What are the clinical implications?

- Considering the evolutionary conservation of *Ahit* across various species, including mouse, rat, and human, the identification of human *Ahit* analog LUNAR1 and its overexpression in the serum samples of patients diagnosed with hypertensive heart diseases, advocates the relevance of *Ahit* as a potential therapeutic target for the treatment of cardiac hypertrophy.

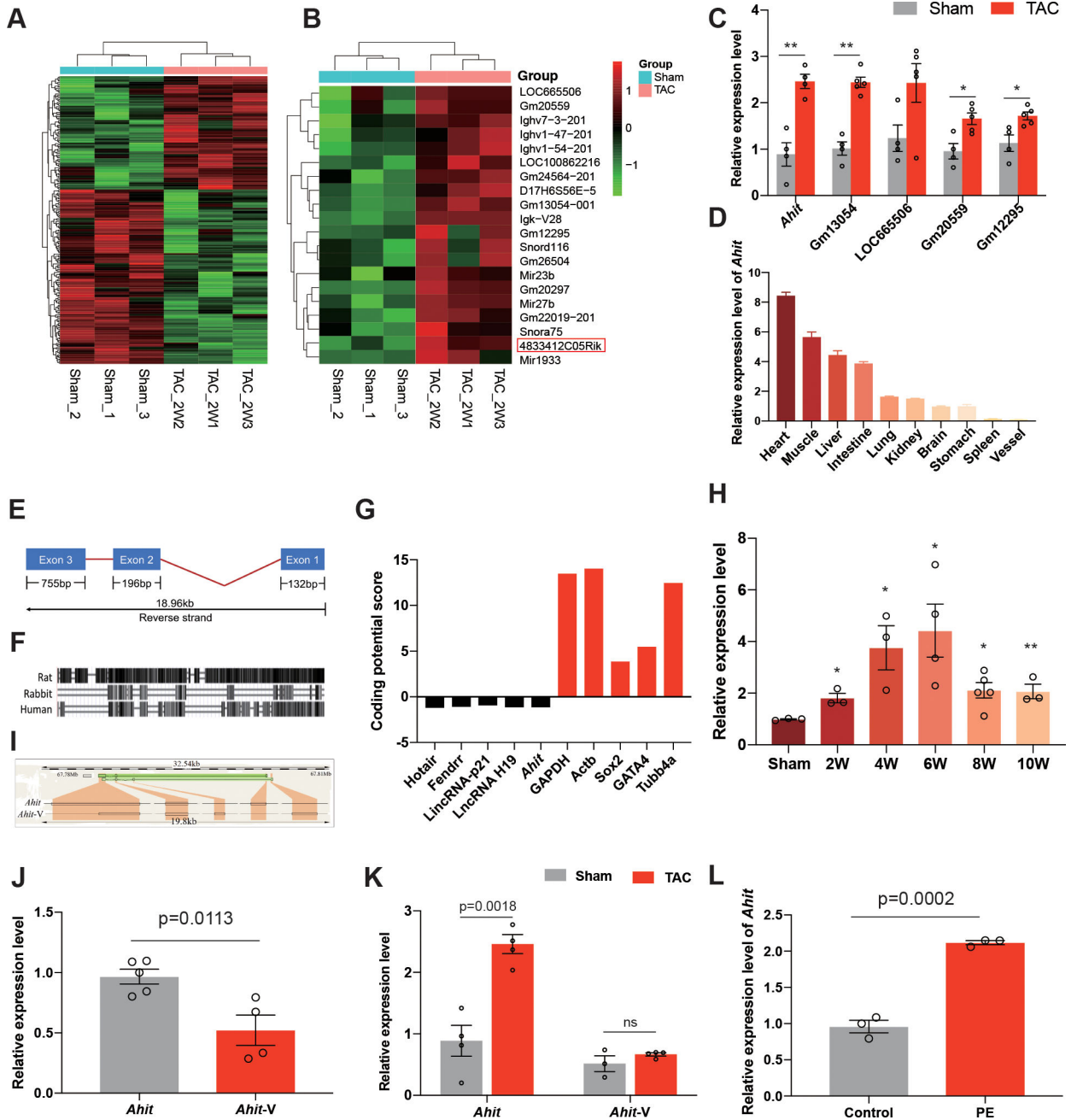


**Figure 1. Profile of the long non-coding RNA *Ahit*.**

**A.** Hierarchical clustering of 239 differentially expressed ncRNAs in hearts of sham and TAC mice (n=3, fold-change > 1.2,  $P < 0.05$ ). **B.** Heat map of the top 20 up-regulated ncRNAs in hearts of TAC mice, compared with sham control mice. *Ahit* (4833412C05Rik) is boxed-in. **C.** qRT-PCR validation of *Ahit*, Gm13054, LOC665506, Gm20559, and Gm12295, the most highly expressed ncRNAs, among the 20 up-regulated ncRNAs in hearts of TAC mice, relative to sham control mice which were given a value of 100% (n=5/group,  $**P < 0.01$ ;  $*P < 0.05$  versus sham). **D.** Relative expression of *Ahit* mRNA quantified by qRT-PCR in various tissues (n=3). **E.** Schematic diagram of *Ahit*. The exons and length are

indicated. **F.** Conservation of *Ahit* in the mouse, rat, rabbit, and human. The horizontal lines indicate the mouse *Ahit* while the black boxes are *Ahit* conserved sequences in rat, rabbit, and human. **G.** The protein-coding potential of *Ahit*, calculated by Protein Coding Potential Calculator, compared with well-established lncRNAs and protein coding genes; *Ahit* and the known lncRNAs have negative values. **H.** The time-course expression of *Ahit* in sham (n=3) and following TAC of 2 weeks (n=3), 4 weeks (n=3), 6 weeks (n=4), 8 weeks (n=5) and 10 weeks (n=3),  $**P < 0.01$ ;  $*P < 0.05$  versus sham. **I.** Schematic illustration of *Ahit* and its splicing variant, *Ahit-V*, in the mouse chromosome. **J.** Abundance of the two transcripts, *Ahit* and *Ahit-V*, in mouse hearts under normal conditions (n=5/group). **K.** qRT-PCR of the two *Ahit* transcripts in hearts from sham and TAC mice (n=4). **L.** *Ahit* mRNA, quantified by qRT-PCR, in NRCMs treated with vehicle (control) or PE (10  $\mu$ M) for 48h (n=3). Data are shown as mean $\pm$ SEM.

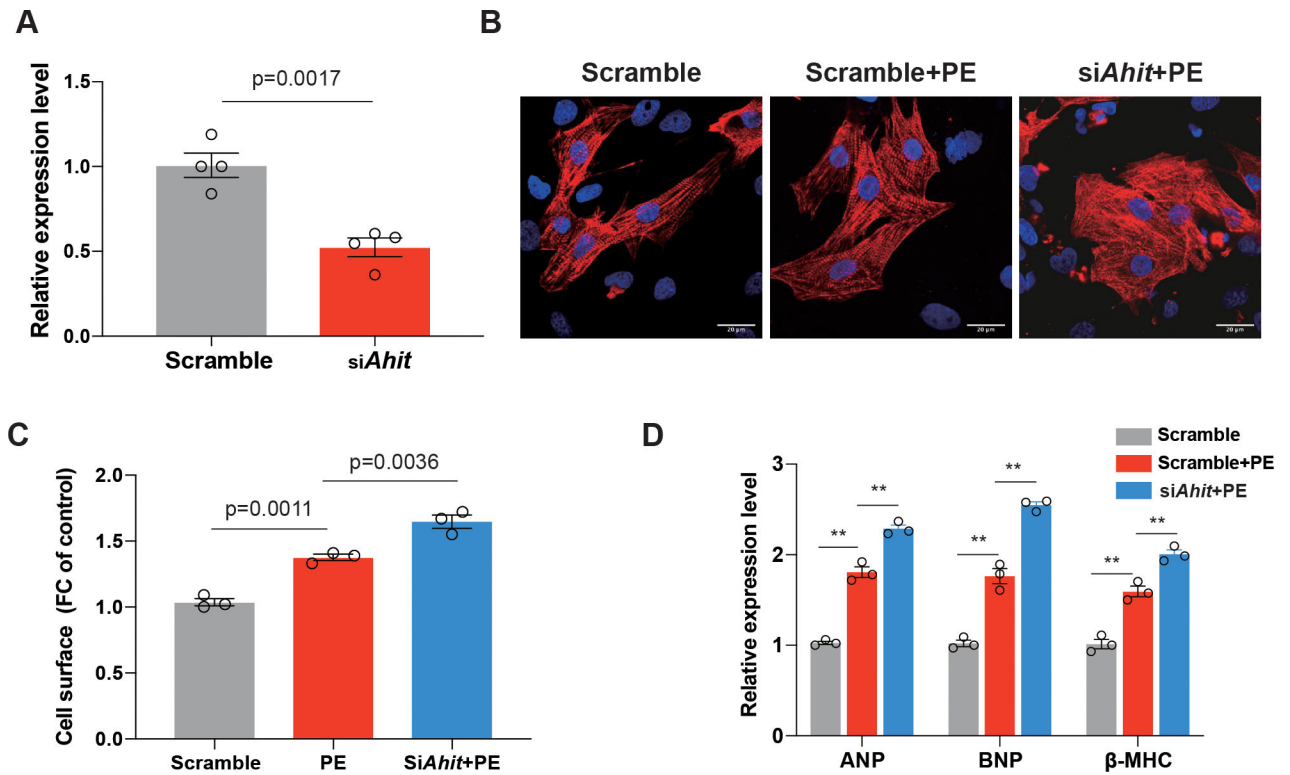


**Figure 2. Downregulation of *Ahit* promotes PE-induced cardiomyocyte hypertrophy.**

**A.** *Ahit* expression in NRCMs transfected with siRNA targeting *Ahit* (*siAhit*) or control siRNA (scramble) for 24 h ( $n=4$ ). **B-D.** Effect of PE (10  $\mu$ M/48h) in NRCMs (NRCMs were not used because they do not hypertrophy in response to PE, data not shown) pretreated with *siAhit* (*SiAhit+PE*) or scramble siRNA (*Scramble+PE*). Another group of NRCMs were treated with scramble siRNA but not PE (scramble). Representative immunohistochemistry images of NRCMs stained with  $\alpha$ -actinin in red and 4',6-diamidino-2-phenylindole (DAPI) in blue. **(B).** Fold-change of the cell surface area of  $\alpha$ -actinin-positive NRCMs ( $n=3$  slides with 10 fields/slide, one-way ANOVA, Holm-Sidak test) **(C).** The mRNA expressions of hypertrophy marker genes ANP, BNP, and  $\beta$ -MHC in NRCMs were quantified by qRT-PCR ( $n=3$ ,  $**P < 0.01$  versus scramble or scramble+PE, one-way ANOVA, Holm-Sidak test) **(D).** Data are shown as mean $\pm$ SEM.



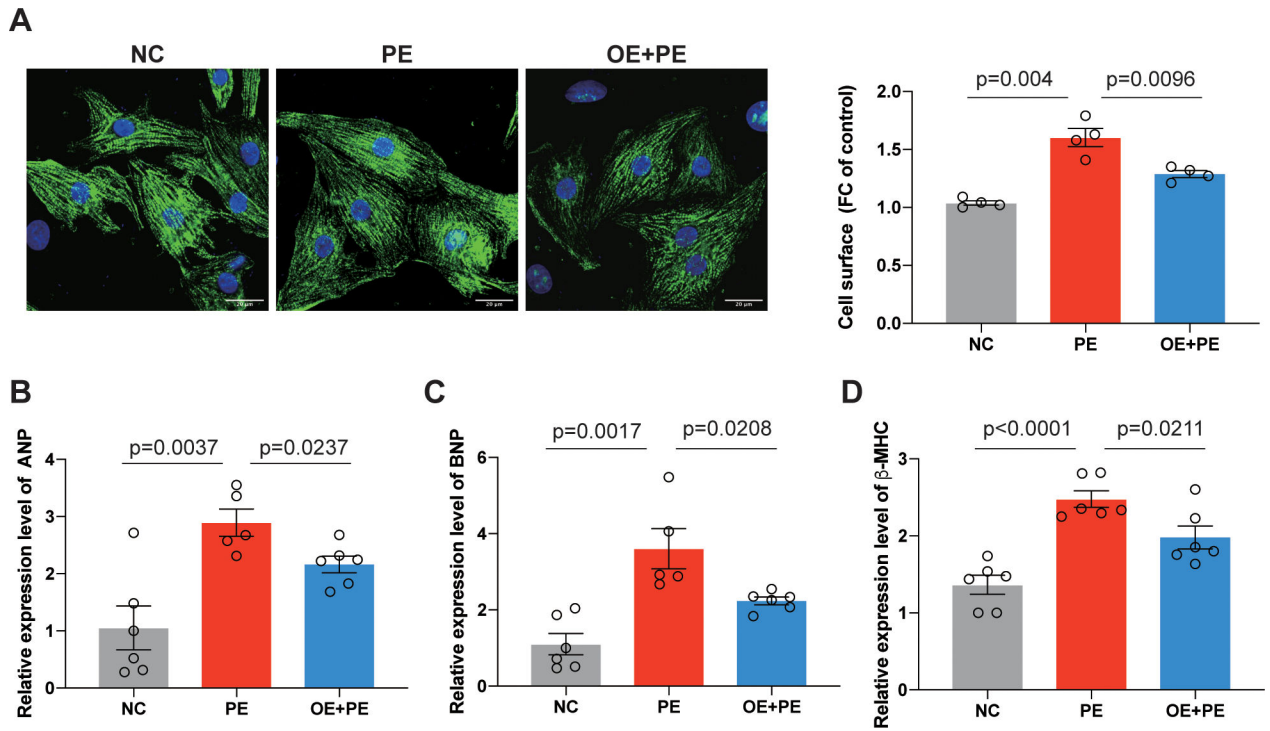


**Figure 3. *In vitro* overexpression of *Ahit* represses PE-induced cardiomyocyte hypertrophy.**

**A.** Representative images (left) and analysis (right) of the cell surface area of NRCMs (cTNT-positive) in the indicated groups ( $n=4$  slides with 10 fields/slide, one-way ANOVA, Holm-Sidak test). **B-D.** The mRNA expressions of hypertrophy marker genes ANP (B), BNP (C), and  $\beta$ -MHC (D) in NRCMs were quantified by qRT-PCR ( $n=6$ , one-way ANOVA, Holm-Sidak test). Data are shown as mean $\pm$ SEM. NC: negative control, PE: phenylephrine, OE: *Ahit* overexpression.

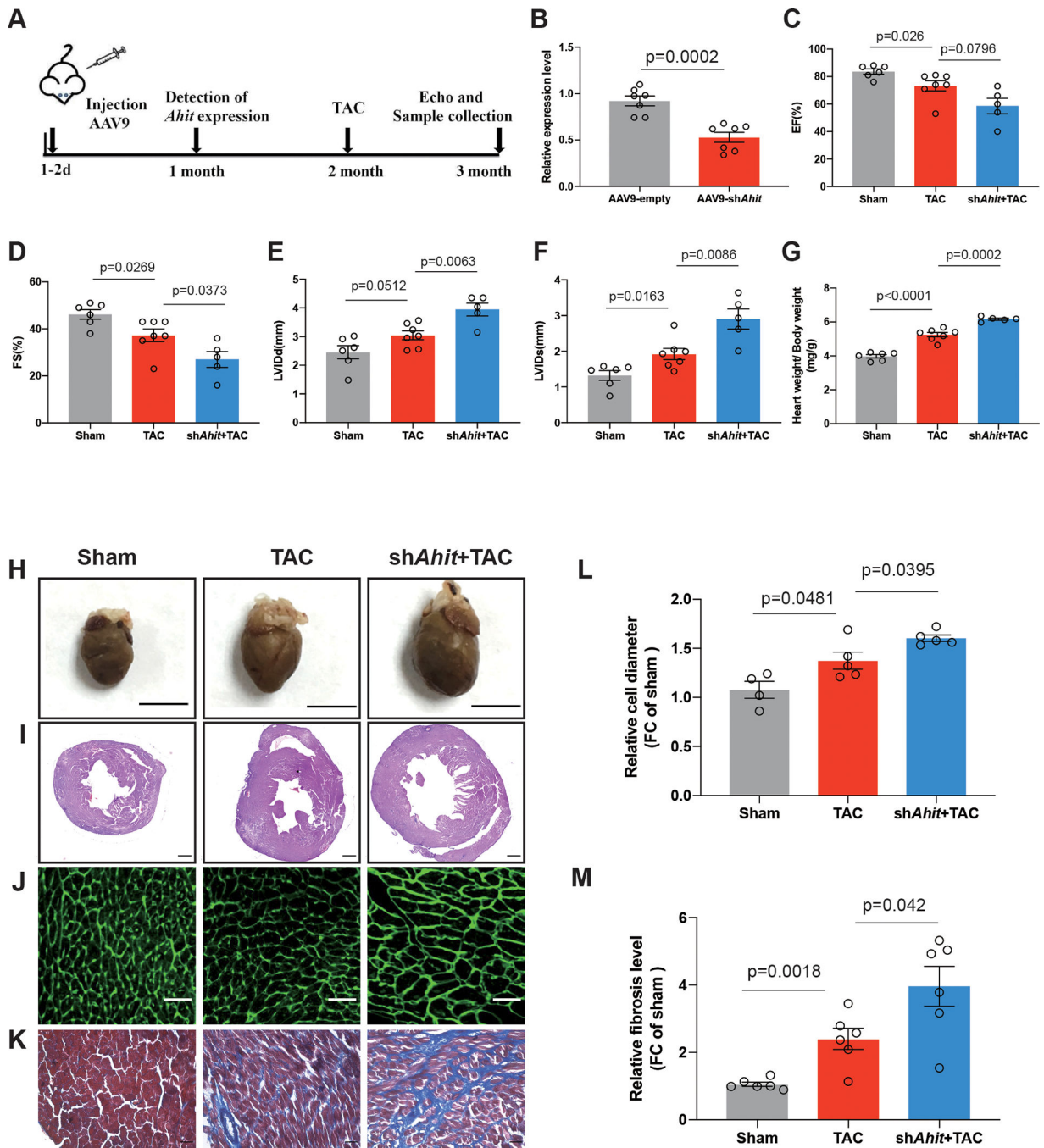


**Figure 4. *Ahit* knockdown aggravates pressure overload-induced cardiac hypertrophy.**  
**A.** Schematic illustration of the experimental design with AAV9 injections targeting *Ahit* (AAV9-sh*Ahit*) or control (AAV9-empty). Neonatal C57Bl/6J mice were infected with a single intraperitoneal injection of AAV9-sh*Ahit* or AAV9-empty. The expression of *Ahit* was detected one-month post injection. Sham or TAC surgeries were performed at 2 months of age in infected mice. **B.** Myocardial *Ahit* expression in mice infected with AAV9-sh*Ahit* or AAV9-empty ( $n=7$  mice/group, Student's t-test). **C-G.** Echocardiography analyses of cardiac function and ratio of heart weight to body weight one month after TAC. EF: Left ventricular

ejection fraction; FS: Fractional shortening; LVIDd: Left ventricular internal dimension at end-diastole; LVIDs: Left ventricular internal dimension at end-systolic pressure ( $n=7$  mice/group, one-way ANOVA, Holm-Sidak test). **H.** Representative macroscopic appearance of the heart in the indicated groups one month after TAC or sham. **I-K.** Representative images of hematoxylin-Eosin (**I**), Wheat Germ Agglutinin (WGA) (**J**), and Masson (**K**) staining of hearts from AAV9-empty or sh*Ahit* mice, one month after TAC or sham ( $n=7$ /group). **L:** Quantification of the cardiomyocyte diameters in WGA staining in Figure **J** ( $n=7$  /group with 10 fields/condition, one-way ANOVA, Holm-Sidak test). **M:** Quantification of fibrosis in Masson staining in Figure **K** ( $n=7$ /group with 10 fields/condition, one-way ANOVA, Holm-Sidak test). Data are shown as mean $\pm$ SEM.

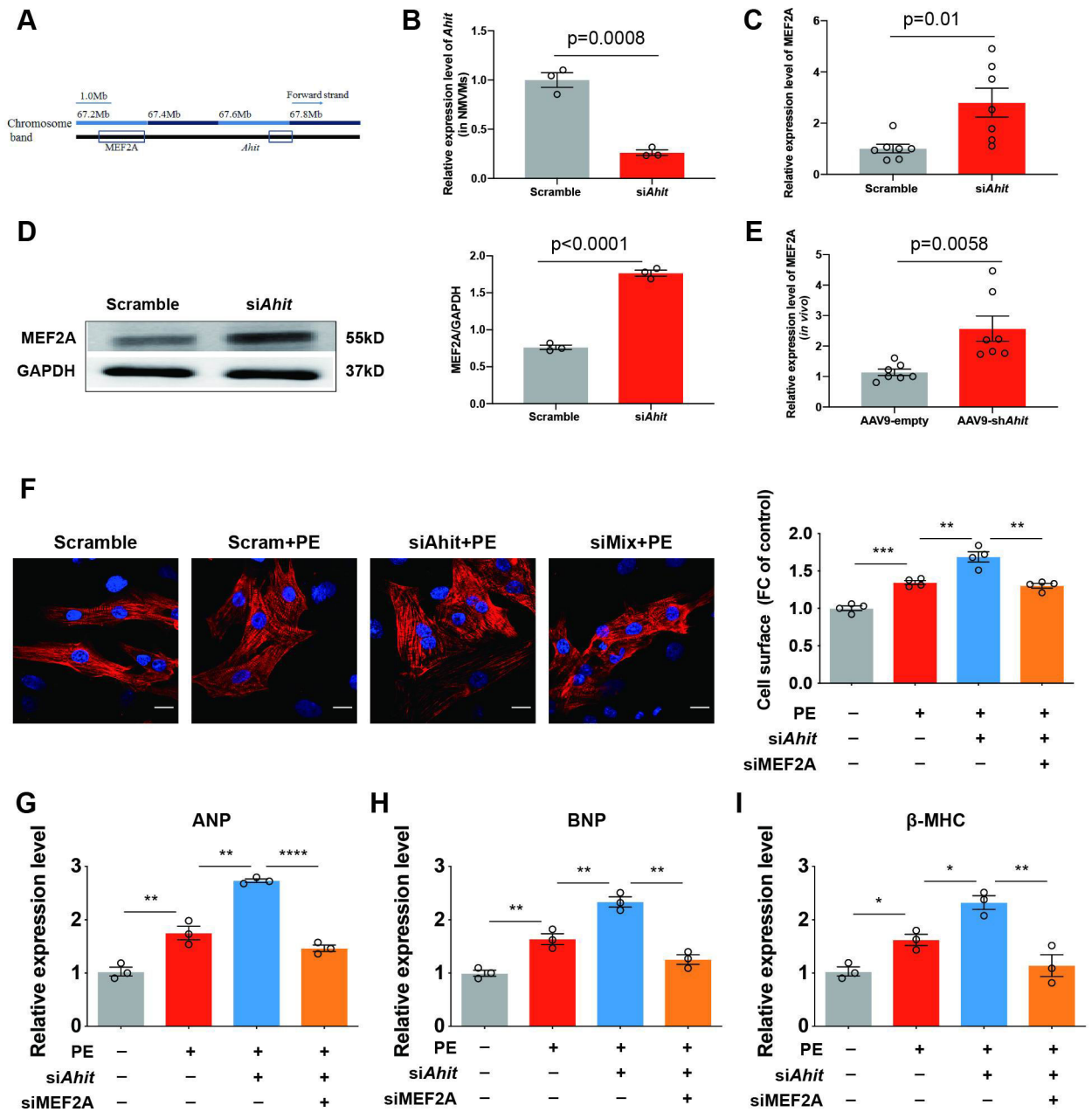


**Figure 5. *Ahit* negatively regulates cardiac hypertrophy through MEF2A *in vitro* and *in vivo*.**  
**A.** Schematic representation of *Ahit* locus and the adjacent MEF2A gene in mouse chromosome 7. **B.** Reduced expression of *Ahit* in NCMs treated with *Ahit* siRNA ( $n=3$ , Student's t-test). **C and D.** qRT-qPCR (**C**) and western blotting (**D**) analyses of MEF2A expression in the NCMs transfected with *Ahit* or scramble siRNA ( $n=3$ , Student's t-test). Data are shown as mean $\pm$ SEM. **E.** Cardiac *in vivo* expression of MEF2A in AAV9-sh*Ahit* infected mice detected by RT-qPCR ( $n=7$ , Student's t-test). **F-I.** NRCMs were transfected with *Ahit* siRNA alone or with MEF2A siRNA, followed by treatment with PE (10  $\mu$ M, 48 h). Representative images (**F** left) and analysis of the cell surface area (right) of NRCMs stained with  $\alpha$ -actinin (red) and DAPI (blue) ( $n=4$  slides/group with 10 fields/slide,  $**P <$

0.01,  $***P < 0.001$  versus the compared group, one-way ANOVA, Holm-Sidak test). mRNA expressions of ANP (**G**), BNP (**H**), and  $\beta$ -MHC (**I**). ( $n=3$ ,  $**P < 0.01$ ,  $****P < 0.0001$  versus the compared group, one-way ANOVA, Holm-Sidak test). Data are shown as mean  $\pm$ SEM.

Author Manuscript

Author Manuscript

Author Manuscript

Author Manuscript

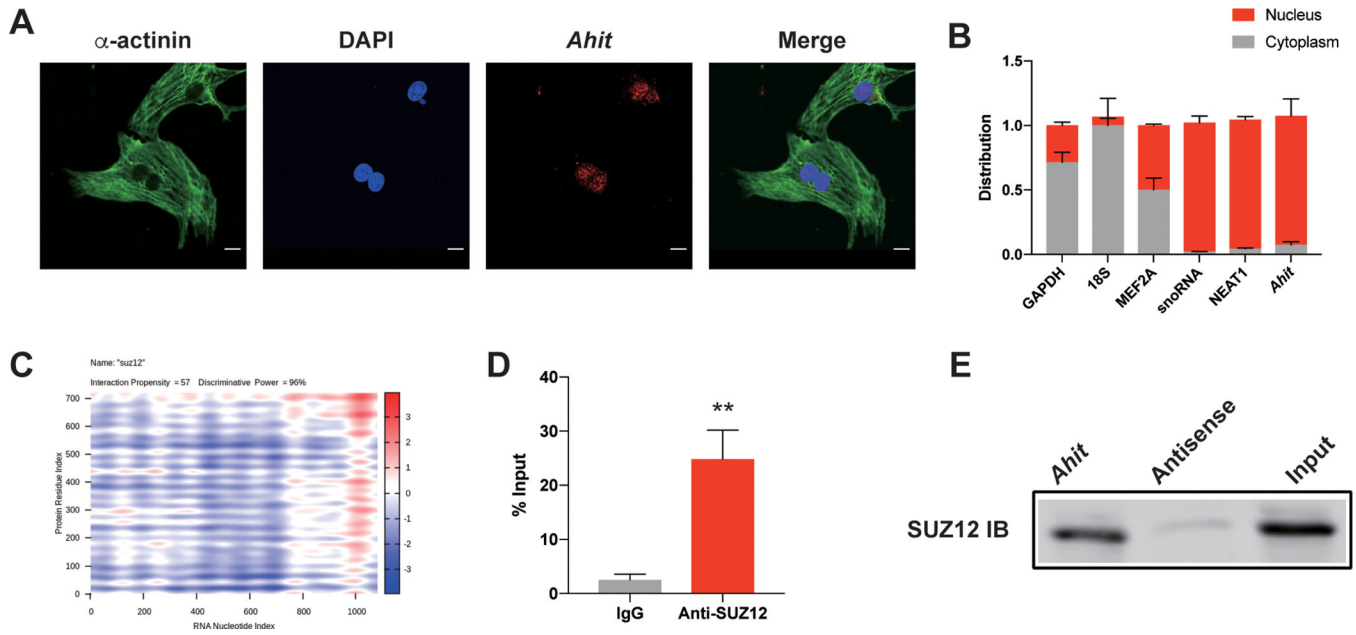


**Figure 6. *Ahit* is a nuclear lncRNA and interacts with SUZ12.**

**A.** RNA fluorescence *in situ* hybridization (FISH) assays of *Ahit* (red) in NMCMs;  $\alpha$ -actinin is green, nucleus (DAPI) is blue. **B.** Percentage of nuclear (blue bar) and cytoplasmic (red bar) RNA concentrations of *Ahit* relative to GAPDH and 18S (cytoplasmic markers), and snoRNA and NEAT1 (nuclear markers) quantified by qRT-PCR. Results (mean $\pm$ SEM) are expressed as relative proportions ( $n=3$ ). **C.** Online- predicted interaction between *Ahit* and SUZ12 on catRAPID website. Red represents interaction strength. **D.** RNA immunoprecipitation (RIP) of SUZ12 and *Ahit* in NMCMs. Bars represent fold -enrichment of *Ahit* immunoprecipitated by specific SUZ12 antibody or anti-IgG ( $n=4$ , \*\* $P < 0.01$  versus IgG, Student's t-test). Data are shown as mean $\pm$ SEM. **E.** Representative immuno-blotting of SUZ12 pulled down from biotinylated *Ahit* incubated with nuclear extracts of NMCMs (repeated for 4 times). Antisense RNA was set as negative control.



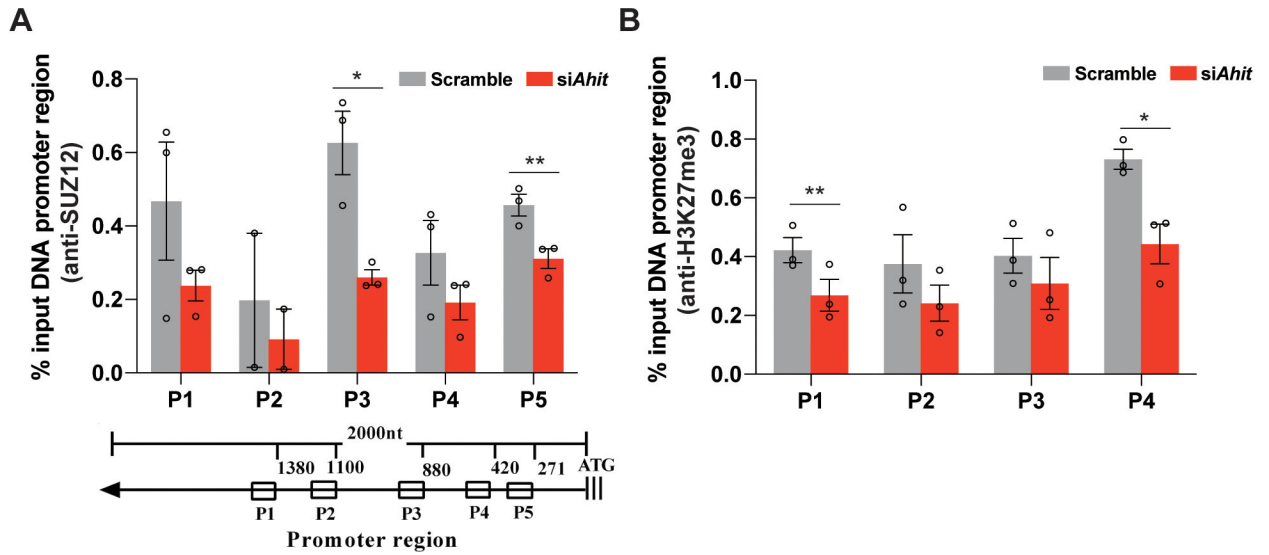


**Figure 7. *Ahit* regulates PRC2 occupancy on the MEF2A promoter locus and H3K27me3 accumulation.**

**A.** Chromatin immunoprecipitation (ChIP) was performed in NMCs using anti-SUZ12 antibody. Five primers, P1-P5, were designed to cover the 1500 bp of MEF2A promoter region. Enrichment was normalized with input, IgG ChIP was used as negative control ( $n=3$ ,  $*P < 0.05$ ,  $**P < 0.01$  versus scramble, Student's t-test). **B.** ChIP-qPCR of H3K27me3 modification at the promoter region of the MEF2A locus after *Ahit* or scramble siRNA in NMCs. Antibody against H3K27me3 was used ( $n=3$ ,  $*P < 0.05$ ,  $**P < 0.01$  versus scramble, Student's t-test). Data are shown as mean $\pm$ SEM.

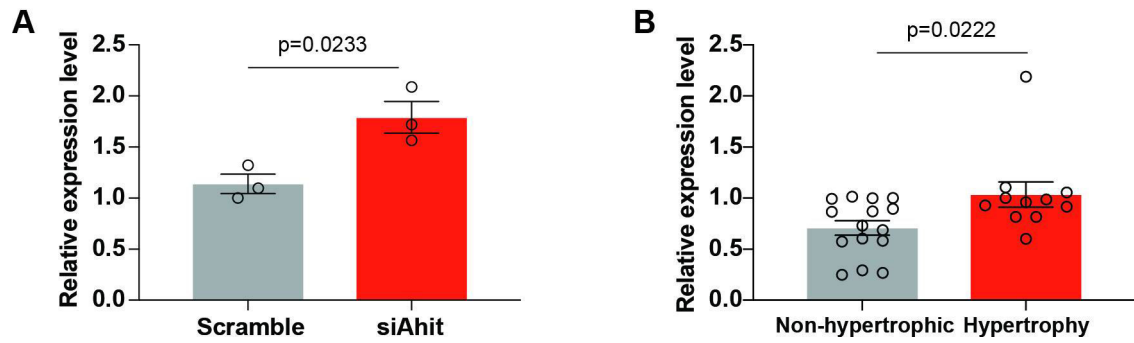


**Figure 8. *Ahit* is correlated with cardiac hypertrophy in human.**

**A.** MEF2A expression in human aortic smooth muscle cells transfected with scramble or siRNA targeting LUNAR1, the human homologous *Ahit* ( $n=3$ , Student's t-test). **B.** The expression of LUNAR1 in serum of patients with cardiac hypertrophy ( $n=12$ ) and healthy control ( $n=16$ , Mann Whitney test). Data are shown as mean±SEM.

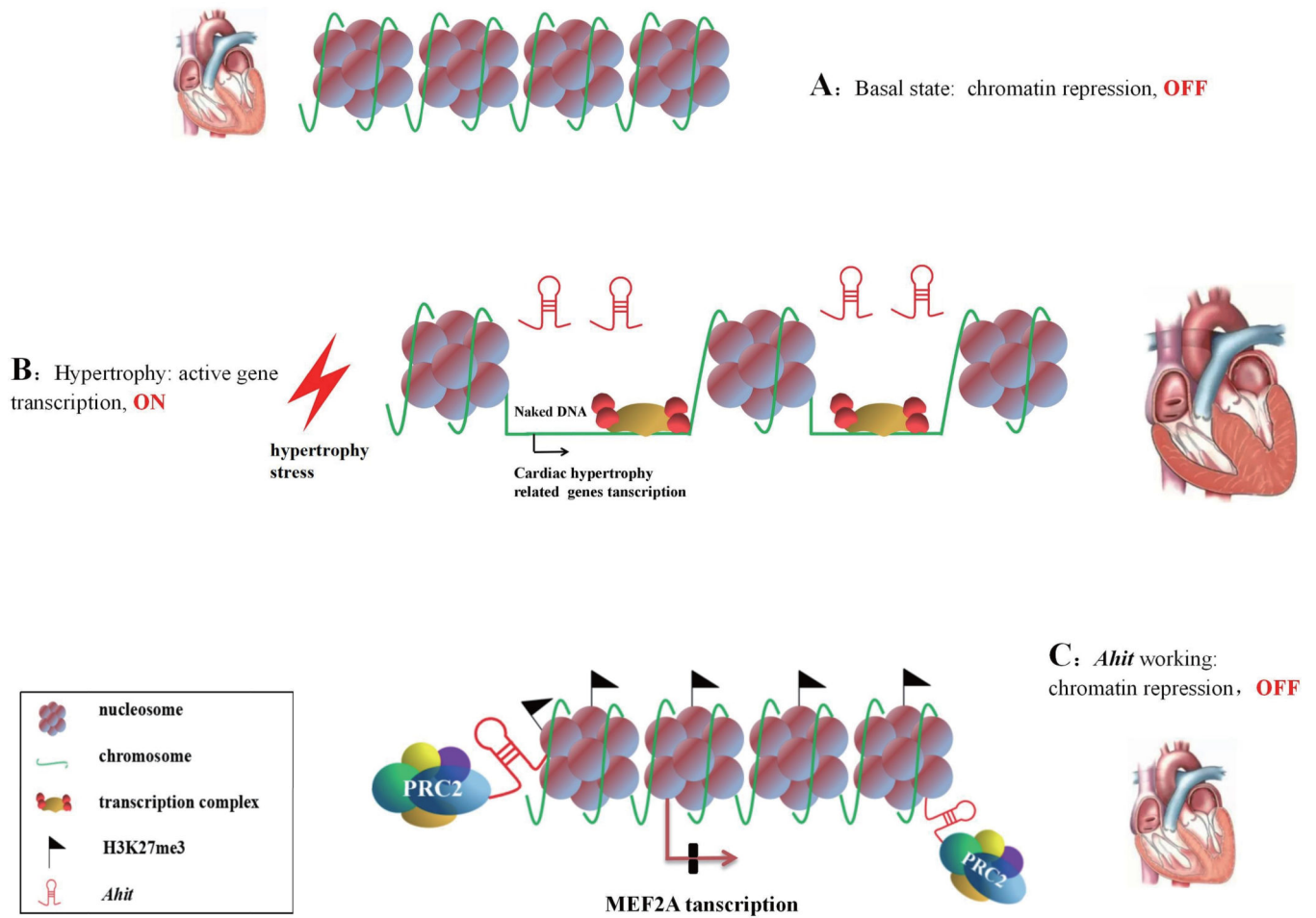


**Figure 9. Proposed working model of *Ahit* in cardiac hypertrophy.**

**A.** Under normal condition the chromatin structure is dense and hypertrophy gene transcriptions are repressed, resulting in OFF status. **B.** The chromatin structure loosens in response to hypertrophy stress, leading to the binding of naked DNA and transcription complex, which accelerates hypertrophy genes transcription, resulting in ON status. **C.** *Ahit* recruits PRC2 complex to induce H3K27me3 in MEF2A promoter, acting as a scaffold, and modulates chromatin remodeling in the dense state, preventing transcription of hypertrophy genes, resulting in prevention of cardiac hypertrophy.